

Superconductor-to-metal quantum phase transition in overdoped $\text{La}_{2-x}\text{Sr}_x\text{CuO}_4$

T. R. Lemberger,^{1,*} I. Hetel,¹ A. Tsukada,² M. Naito,² and M. Randeria¹

¹*Department of Physics, The Ohio State University, Columbus, Ohio 43210, USA*

²*Tokyo University of Agriculture and Technology, Tokyo, Japan*

(Received 29 March 2011; published 20 April 2011)

We investigate T_c and magnetic penetration depth $\lambda(T)$ near the superconductor-metal quantum phase transition in overdoped $\text{La}_{2-x}\text{Sr}_x\text{CuO}_4$ films. Both T_c and superfluid density n_s , $\propto \lambda^{-2}$, decrease with overdoping. They obey the scaling relation $T_c \propto [\lambda^{-2}(0)]^\alpha$ with $\alpha \approx 1/2$. We discuss this result in the frameworks of disordered d -wave superconductors and of scaling near quantum critical points. Our result, and the linear scaling ($\alpha \approx 1$) found for the more anisotropic $\text{Tl}_2\text{Ba}_2\text{CuO}_{6+\delta}$, can both be understood in terms of quantum critical scaling, with different dimensionalities for fluctuations.

DOI: [10.1103/PhysRevB.83.140507](https://doi.org/10.1103/PhysRevB.83.140507)

PACS number(s): 74.40.Kb, 74.25.Dw, 74.25.fc, 74.72.Gh

The superconductor-to-nonsuperconductor transitions in cuprates, as functions of carrier concentration, give insights into quantum phase transitions (QPTs) in general¹ and into the phenomenon of high-temperature superconductivity in particular.²⁻⁴ On the underdoped side, the transition is from superconducting to an insulating state with a (pseudo)gap in the electronic excitation spectrum that remains finite through the QPT. The fundamental physics on the overdoped side of the phase diagram is profoundly different because there is no pseudogap, the superconducting gap becomes progressively smaller⁵ with doping, and the QPT is from superconductor to a metal that is similar to a conventional Fermi liquid in many respects.

Key issues are as follows: (i) Are these transitions first order or are they quantum critical points (QCPs) where quantum fluctuations of the order parameter are important? (ii) How does the presence or absence of an energy gap impact the transitions? (iii) Are these transitions driven by a collapse of the pairing amplitude or by fluctuations of the phase of the superconducting order parameter? (iv) Does anisotropy (c axis vs ab plane) affect the dimensionality of the QCPs?

T_c as a function of hole doping p takes a quasiuniversal form,⁶ with superconductivity existing for $0.03 \lesssim p \lesssim 0.30$, with a maximum at $p \approx 0.15$, independent of the maximum value of T_c or of c vs ab -plane anisotropy. Thus, one might expect a common explanation for the over- and underdoped quantum phase transitions in different compounds.

An early study of several underdoped cuprate compounds suggested that T_c and superfluid density ($n_s \propto \lambda^{-2}$, $\lambda =$ magnetic penetration depth) might be linearly proportional, $T_c \propto \lambda^{-2}(0)$, with a universal slope as critical underdoping is approached.⁷ This linear scaling led to the widely accepted view that classical thermal phase fluctuations destroy superconductivity⁴ in underdoped cuprates when the superfluid density becomes small, even as the energy gap remains intact. This long-standing view was overturned recently by measurements on severely underdoped $\text{YBa}_2\text{Cu}_3\text{O}_{7-\delta}$ (YBCO) films⁸ and crystals,⁹ showing that scaling is actually sublinear, $T_c \propto [\lambda^{-2}(0)]^\alpha$ with $\alpha \approx 0.5$. Sublinear scaling, together with the absence of critical thermal fluctuations near T_c , pointed to a three-dimensional (3D) QCP.^{2,3} The QCP hypothesis was put to a stringent test in a study of two-unit-cell-thick underdoped YBCO films that were two dimensional (2D) by construction. Indeed, linear scaling expected near a 2D QCP was observed for these ultrathin films.¹⁰

The present work focuses on the *overdoped* QPT in $\text{La}_{2-x}\text{Sr}_x\text{CuO}_4$ (LSCO). While the underdoped regime has been explored in several materials, studies in the overdoped regime have focused largely on a single material: $\text{Tl}_2\text{Ba}_2\text{CuO}_{6+\delta}$ (Tl2201).^{11,12} We are motivated to study LSCO because it can be doped through both over- and underdoped quantum phase transitions, and it is much less anisotropic than Tl2201, thus allowing us to address the key question of the effective dimensionality of fluctuations. Our main results are as follows:

(1) All overdoped samples with high Sr concentrations, $x > 0.22$, have sharp superconducting-to-normal thermal phase transitions, as narrow as 200 mK near the QPT. This suggests that the overdoped QPT is not dominated by inhomogeneity or phase separation.

(2) Near the overdoped QPT, we find sublinear scaling $T_c \propto [\lambda^{-2}(0)]^\alpha$ with $\alpha \approx 0.5$ for LSCO, in contrast to the linear scaling ($\alpha \approx 1.0$) seen in Tl2201.^{11,12}

(3) We argue that scaling with $\alpha \approx 0.5$ is consistent with either (a) a mean-field QPT driven by gap collapse in a disordered d -wave superconductor, or (b) a 3D QCP. In case (a), asymptotically close to the QPT one must take into account critical fluctuations. Case (b) permits us to reconcile the square-root scaling in LSCO with the linear scaling in Tl2201.

Our $\text{La}_{2-x}\text{Sr}_x\text{CuO}_4$ films were grown by MBE on (001) LaSrAlO_4 (LSAO) substrates¹³ (see Table I). The films' c axes are perpendicular to the substrate. Compressive strain due to a small lattice mismatch (-1.28% at $x = 0$; -0.6% at $x \approx 0.15$; and -0.28% at $x \approx 0.30$)¹⁴ gives our films a maximum T_c (≈ 44 K) that is slightly higher than the maximum T_c (≈ 38 K) of LSCO crystals. Based on the small effect of strain on the maximum T_c and superfluid density of our films relative to bulk, and other similarities between films and bulk samples described in the following, we believe that the overall effect of strain on our films is small. Sr doping values are nominal. They are set by atomic beam fluxes during deposition.

After the first series of films (thickness $d = 45$ nm) was grown, noting the jump in properties between $x = 0.24$ and $x = 0.27$, we decided to grow a film at $x = 0.30$ and a second film at $x = 0.27$ (both with $d = 90$ nm) to get more data points near the QPT. (See the last two rows of Table I.) These films were grown with a slightly different protocol, aimed at keeping oxygen stoichiometry at 4.0, and with a greater thickness since

TABLE I. Properties of $\text{La}_{2-x}\text{Sr}_x\text{CuO}_4$ films grown by MBE on LSAO (100). x values are nominal. The last two films were grown well after the others with a slightly different protocol, and they are twice as thick.

x	$T_c(\rho_{ab})$ (K)	$T_c(\lambda^{-2})$ (K)	$\lambda^{-2}(0)(\mu\text{m}^{-2})$	ρ_{ab} (50 K) ($\mu\Omega$ cm)
0.06	17.5	16	1.3	590
0.06	24	23	4.5	377
0.09	39.7	33	6	170
0.09	40	38	10.5	160
0.12	40.1	39	12.5	140
0.15	44	42	17.4	90
0.18	41	38	21.5	54
0.21	33	32	20.3	48
0.24	19	18.5	11.1	37
0.27	4.0	3.9	0.15	31
0.27	21	20	3.4	70
0.30	9	8.5	0.8	56

that change seemed to improve film properties somewhat. They have somewhat higher T_c 's and superfluid densities than for the first series, perhaps due in part to a slight difference in oxygenation.

Two samples were grown simultaneously at each Sr concentration, one on a narrow substrate for measuring resistivity and the other on a $10 \times 10 \times 0.35$ mm³ substrate for measuring λ^{-2} . Sheet conductivity, $\sigma d = \sigma_1 d - i\sigma_2 d$, was measured with a low-frequency ($\omega/2\pi = 50$ kHz) two-coil mutual inductance technique, with drive and pickup coils on opposite sides of the film.¹⁵ Near T_c , the real part of the conductivity $\sigma_1(T)$ has a peak that probes the spatial homogeneity of T_c . The imaginary part, $\sigma_2(T)$, yields the magnetic penetration depth λ via $\lambda^{-2}(T) \equiv \mu_0\omega\sigma_2(T)$. $\lambda^{-2}(T)$ is often loosely referred to as “superfluid density” n_s since the two are proportional.

The ab -plane resistivities of our films decrease smoothly with doping (Fig. 1), achieving a low residual resistivity of about 40 $\mu\Omega$ cm at the highest doping, comparable to that of a similarly overdoped LSCO crystal.¹⁶ T_c , defined from where

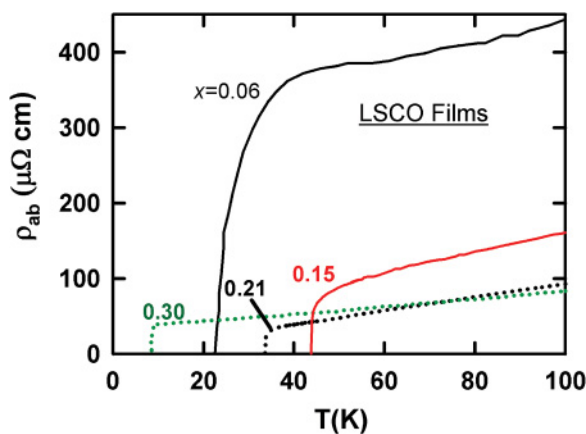


FIG. 1. (Color online) ab -plane resistivity $\rho_{ab}(T)$ for typical $\text{La}_{2-x}\text{Sr}_x\text{CuO}_4$ films, $x = 0.06, 0.15, 0.21, 0.30$, illustrating the shallow minimum in resistivity and the maximum in T_c as functions of doping.

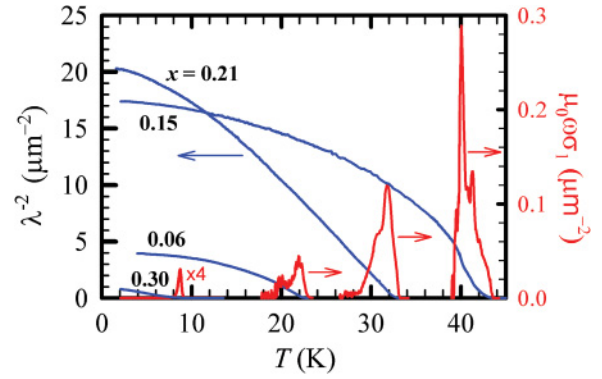


FIG. 2. (Color online) $\lambda^{-2} \equiv \mu_0\omega\sigma_2$ (blue curves) and $\mu_0\omega\sigma_1(T)$ (red peaks) measured at $\omega/2\pi = 50$ kHz for $\text{La}_{2-x}\text{Sr}_x\text{CuO}_4$ films, $x = 0.06, 0.15, 0.21, 0.30$, illustrating the maxima in T_c and $\lambda^{-2}(0)$ as functions of doping.

ρ_{ab} vanishes, agrees within a kelvin or so with T_c defined from where superfluid appears.

Peaks in $\sigma_1(T)$ (Figs. 2 and 3) probe film homogeneity. Films with $x \leq 0.21$ have narrow peaks, but with structure indicating the presence of several closely-spaced T_c 's over the mm-scale area probed. On the other hand, films with $x \geq 0.24$ have single peaks ~ 1 K wide, e.g., the $x = 0.30$ film in Fig. 2. The peak is only 0.2 K wide for the film closest to the QPT (Fig. 3), consistent with good film homogeneity, although there are other experiments¹⁷ suggesting a phase-separated overdoped superconducting state. σ_1 is plotted as $\mu_0\omega\sigma_1$ ($\mu_0 =$ permeability of vacuum $= 4\pi \times 10^{-7}$ H/m) to facilitate quantitative comparison with $\lambda^{-2} \equiv \mu_0\omega\sigma_2$.

Figures 2 and 3 show $\lambda^{-2}(T)$ for representative LSCO films, illustrating the interesting qualitative feature that $\lambda^{-2}(T)$ for overdoped films has a less downward curvature than for underdoped and optimally doped films. The same qualitative effect is seen in LSCO powders¹⁸ and in Tl2201 powders.^{11,12,17}

T_c vs x for films (black squares in Fig. 4) has the same overall behavior as bulk LSCO,¹⁹ and many other cuprate compounds,⁶ rising from zero at $x \approx 0.055$, peaking at $x \approx 0.15$ and vanishing again at $x \approx 0.30$. $\lambda^{-2}(0)$ vs x for films (red squares in Fig. 4) tracks that of LSCO powders (green circles)¹⁹ up to $x \approx 0.18$. $\lambda^{-2}(0)$ of our films decreases with further overdoping, peaking near $x \approx 0.19$, consistent with many

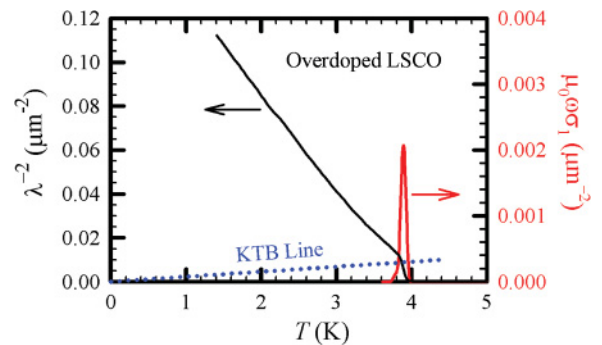


FIG. 3. (Color online) $\lambda^{-2}(T)$ (black curve) and $\mu_0\omega\sigma_1(T)$ (red peak) for an overdoped LSCO film very close to the QPT. The KTB line (blue dotted) is calculated assuming the film fluctuates as a single 2D entity.

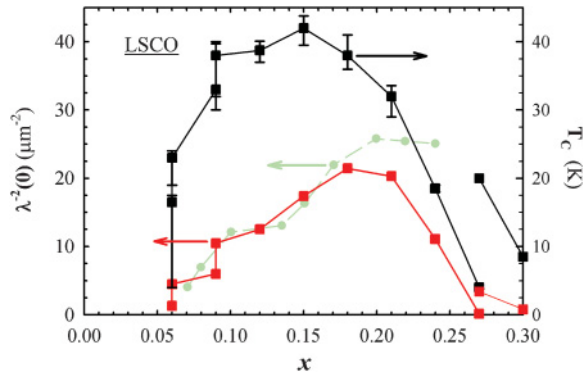


FIG. 4. (Color online) T_c (black squares) and $\lambda^{-2}(0)$ (red (gray) squares) vs x for LSCO films; $\lambda^{-2}(0)$ vs x for LSCO powders (green dots).¹⁸

other bulk cuprate compounds^{11,12,20} and with other LSCO films.²¹ We cannot explain why $\lambda^{-2}(0)$ in LSCO powders¹⁹ does not decrease for $x > 0.19$. Resistivity and superfluid density measurements show that our films are essentially of the same quality as bulk cuprates.

A detailed examination of how the magnitude and T dependence of superfluid density change across the phase diagram is presented elsewhere.²² Here we focus on scaling of T_c vs $\lambda^{-2}(0)$ (Fig. 5). Data from our under- and overdoped LSCO films are shown as open and filled red squares, respectively. Data on other cuprates^{8,10} are shown for comparison (see the caption). The solid gray line representing square-root scaling is drawn through the underdoped Ca-YBCO thick-film data, but it is close to the underdoped LSCO data, too. The solid

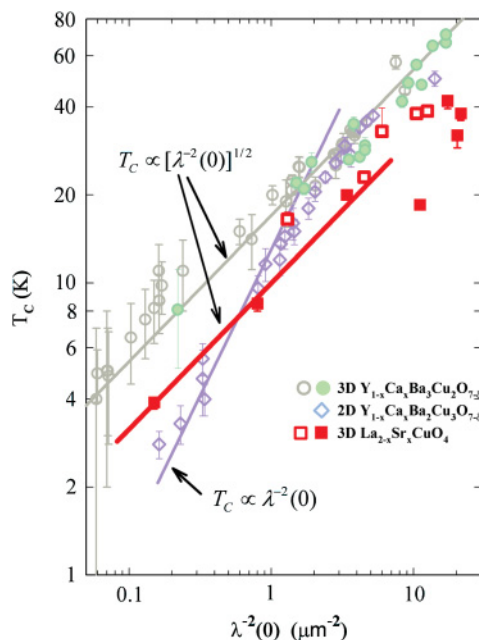


FIG. 5. (Color online) T_c vs $\lambda^{-2}(0)$ for under- and overdoped LSCO films (open and filled red squares, respectively). Also shown are data for 40 unit-cell-thick YBCO⁸ (filled green circles) and Ca-doped YBCO films¹⁰ (open gray circles), and thin underdoped Ca-YBCO films¹⁰ (open purple diamonds), which scale with 3D (2D) exponent $\alpha \approx 1/2$ ($\alpha = 1$). The red line ($\alpha = 1/2$) is drawn through the overdoped LSCO data.

red line representing square root scaling is drawn through the data for strongly overdoped LSCO films. The light blue line representing linear scaling is drawn through the data for two-unit-cell-thick Ca-doped YBCO.

Let us ask *why* n_s decreases with overdoping, even though the carrier density increases. The most natural explanation is the pair-breaking interplay between disorder (scattering rate $1/\tau$) and a d -wave pairing interaction, and thus gap Δ_0 , that weakens with overdoping. (This explanation was anticipated by the generic pair-breaking model proposed in Ref. 12, and is discussed in more detail in Ref. 22.) In a disordered d -wave superconductor, a simple sum-rule argument suggests a linear suppression of $n_s(0)$ to zero with increasing $1/\Delta_0\tau$, which is borne out by detailed calculations.²³ In addition, the dirty d -wave T_c exhibits a square-root suppression to zero with $1/\Delta_0\tau$,²³ so that $T_c \sim [\lambda^{-2}(0)]^{1/2}$. We note this is a mean-field result, and for doping close enough to the QPT, the superfluid density necessarily becomes so small that quantum phase fluctuations dominate the physics. It is not known where the crossover to this asymptotic behavior occurs.

Well-known scaling arguments predict^{1-3,24} that $T_c \sim [\lambda^{-2}(0)]^\alpha$ near a QCP, with exponent $\alpha \equiv z_Q/(z_Q + D - 2)$, where D is the dimensionality and z_Q is the quantum dynamical exponent. Since z_Q should not be less than unity, in $D = 3$ the smallest reasonable exponent is $\alpha = 1/2$, which is coincidentally the same as the dirty- d -wave mean-field result. This describes the observed nonlinear scaling in overdoped LSCO reasonably well.

While the dirty- d -wave and QCP models both capture the square-root scaling of overdoped LSCO, the latter also permits us to understand the linear scaling in overdoped Tl2201,^{11,12} which is much more anisotropic than LSCO and might reasonably display the $D = 2$ exponent of $\alpha = 1$, independent of z_Q . Thus the different scalings seen in LSCO and Tl2201 could be attributed to the different dimensionalities of the fluctuations.

It is worth noting that there is experimental evidence for significant interlayer coupling in overdoped LSCO. Ironically, this evidence comes from a 2D Kosterlitz-Thouless-Berezinski (KTB)-like²⁵ transition seen in the most overdoped film, i.e., the abrupt downturn in λ^{-2} near the intersection of the KTB line with $\lambda^{-2}(T)$ (Fig. 3). The slope of the KTB line in Fig. 3 is calculated assuming that the film fluctuates as a single 2D entity. For independently fluctuating layers, the KTB line would be 70 times steeper. Analogous features appear in microwave measurements of σ in underdoped LSCO films,²⁶ indicating significant interlayer coupling across the LSCO phase diagram. Finally, similar evidence for interlayer coupling is found in “thick” underdoped YBCO films, which also show 3D critical scaling.²⁷

In summary, we observe in overdoped LSCO that superconductivity diminishes, with $T_c \sim [\lambda^{-2}(0)]^{1/2}$. Taken by itself, this behavior may be viewed as a consequence of a mean-field gap collapse in a disordered d -wave superconductor. On the other hand, taken together with the linear scaling in Tl2201, this behavior leads to the interpretation that scaling observed for strongly overdoped samples is due to 3D and 2D quantum critical points, respectively, with the difference in dimensionality due to the much higher anisotropy of Tl2201. Finally, in moderately *underdoped* LSCO we observe sublinear

T_c vs $\lambda^{-2}(0)$ scaling that is quantitatively similar to that of underdoped YBCO. However, data on *severely* underdoped LSCO samples are needed to establish a 3D QCP on the underdoped side.

We acknowledge useful conversations with Ilya Vekhter and David Stroud. This work was supported in part by NSF DMR Grant No. 0203739 (I.H.), DOE Grant No. FG02-08ER46533 (T.R.L.), and NSF-DMR 0706203 (M.R.).

*trl@physics.osu.edu.

- ¹S. Sachdev, *Quantum Phase Transitions* (Cambridge University Press, Cambridge, UK, 1999).
- ²A. Kopp and S. Chakravarty, *Nat. Phys.* **1**, 53 (2005).
- ³M. Franz and A. P. Iyengar, *Phys. Rev. Lett.* **96**, 047007 (2006).
- ⁴V. J. Emery and S. A. Kivelson, *Nature (London)* **374**, 434 (1995).
- ⁵A. Ino, C. Kim, M. Nakamura, T. Yoshida, T. Mizokawa, A. Fujimori, Z. X. Shen, T. Kakeshita, H. Eisaki, and S. Uchida, *Phys. Rev. B* **65**, 094504 (2002).
- ⁶M. R. Presland, J. L. Tallon, R. G. Buckley, R. S. Liu, and N. E. Flower, *Physica C* **176**, 95 (1991).
- ⁷Y. J. Uemura, G. M. Luke, B. J. Sternlieb, J. H. Brewer, J. F. Carolan, W. N. Hardy, R. Kadono, J. R. Kempton, R. F. Kiefl, S. R. Kreitzman, P. Mulhern, T. M. Riseman, D. L. Williams, B. X. Yang, S. Uchida, H. Takagi, J. Gopalakrishnan, A. W. Sleight, M. A. Subramanian, C. L. Chien, M. Z. Cieplak, Gang Xiao, V. Y. Lee, B. W. Statt, C. E. Stronach, W. J. Kosler, and X. H. Yu, *Phys. Rev. Lett.* **62**, 2317 (1989).
- ⁸Y. Zuev, M.-S. Kim, and T. R. Lemberger, *Phys. Rev. Lett.* **95**, 137002 (2005).
- ⁹D. M. Broun, W. A. Huttema, P. J. Turner, S. Ozcan, B. Morgan, R. Liang, W. N. Hardy, and D. A. Bonn, *Phys. Rev. Lett.* **99**, 237003 (2007).
- ¹⁰I. Hetel, T. R. Lemberger, and M. Randeria, *Nat. Phys.* **3**, 700 (2008).
- ¹¹Y. J. Uemura, A. Keren, L. P. Le, G. M. Luke, W. D. Wu, Y. Kubo, T. Manako, Y. Shimakawa, M. Subramanian, J. L. Cobb, and J. T. Markert, *Nature (London)* **364**, 605 (1993).
- ¹²C. Niedermayer, C. Bernhard, U. Binninger, H. Gluckler, J. L. Tallon, E. J. Ansaldo, and J. I. Budnick, *Phys. Rev. Lett.* **71**, 1764 (1993).
- ¹³M. Naito and H. Sato, *Appl. Phys. Lett.* **67**, 2557 (1995); H. Sato and M. Naito, *Physica C* **274**, 221 (1997); H. Sato, A. Tsukada, M. Naito, and A. Matsuda, *Phys. Rev. B* **61**, 12447 (2000); H. Sato, *Physica C* **468**, 2366 (2008).
- ¹⁴A. Tsukada, M. Naito, and H. Sato (unpublished).
- ¹⁵S. J. Turneaure, E. R. Ulm, and T. R. Lemberger, *J. Appl. Phys.* **79**, 4221 (1996); S. J. Turneaure, A. A. Pesetski, and T. R. Lemberger, *ibid.* **83**, 4334 (1998).
- ¹⁶S. Nakamae, K. Behnia, N. Mangkorntong, M. Nohara, H. Takagi, S. J. C. Yates, and N. E. Hussey, *Phys. Rev. B* **68**, 100502(R) (2003).
- ¹⁷Y. J. Uemura, *Solid State Comm.* **120**, 347 (2001).
- ¹⁸C. Panagopoulos, B. D. Rainford, J. R. Cooper, W. Lo, J. L. Tallon, J. W. Loram, J. Betouras, Y. S. Wang, and C. W. Chu, *Phys. Rev. B* **60**, 14617 (1999).
- ¹⁹C. Panagopoulos, T. Xiang, W. Anukool, J. R. Cooper, Y. S. Wang, and C. W. Chu, *Phys. Rev. B* **67**, 220502 (2003).
- ²⁰C. Bernhard, J. L. Tallon, T. Blasius, A. Golnik, and C. Niedermayer, *Phys. Rev. Lett.* **86**, 1614 (2001).
- ²¹J. P. Locquet, Y. Jaccard, A. Cretton, E. J. Williams, F. Arrouy, E. Machler, T. Schneider, O. Fischer, and P. Martinoli, *Phys. Rev. B* **54**, 7481 (1996).
- ²²T. R. Lemberger, I. Hetel, A. Tsukada, and M. Naito, *Phys. Rev. B* **82**, 214513 (2010).
- ²³E. Puchkaryov and K. Maki, *Eur. J. Phys. B* **4**, 191 (1998); Y. Sun and K. Maki, *Phys. Rev. B* **51**, 6059 (1995).
- ²⁴Igor F. Herbut, *Phys. Rev. Lett.* **85**, 1532 (2000).
- ²⁵J. M. Kosterlitz and D. J. Thouless, *J. Phys. C* **6**, 1181 (1973); V. L. Berezinskii, *Zh. Eksp. Teor. Fiz.* **61**, 1144 (1971) [*Sov. Phys. JETP* **34**, 610 (1972)].
- ²⁶H. Kitano, T. Ohashi, A. Maeda, and I. Tsukada, *Phys. Rev. B* **73**, 092504 (2006).
- ²⁷Y. L. Zuev *et al.*, *Physica C* **468**, 276 (2008).